PHYSICAL REVIEW B **68**, 201403(R) (2003)

# Hydrogen effect on adhesion and adhesive transfer at aluminum/diamond interfaces

Yue Qi and Louis G. Hector, Jr.
*Materials and Processes Lab, GM R&D Center, MC: 480-106-224, 30500 Mound Road, Warren, Michigan 48090, USA*
(Received 10 September 2003; published 20 November 2003)

Using a first principles methodology, we find that Al(111)/C(111)-1×1 is energetically favored over Al(111)/C(111)-2×1 even though reconstructed diamond is the stable surface structure. Overlapping Al and diamond *p* states at the unreconstructed interface result in strong adhesion, which leads to an adhesive transfer of two Al layers to the diamond during progressive tensile straining. Decohesion occurs as a jump-to-separate process once the interfacial strength is exceeded. Hydrogen passivation of the diamond leads to negligible adhesion and no transfer of Al.

DOI: 10.1103/PhysRevB.68.201403 PACS number(s): 68.35.Gy

Adhesion and adhesive wear are important to numerous applications in which various loadings are transmitted through different material interfaces. These applications range from microelectronics devices, hard coatings or thermal barrier coatings, where large adhesion is often desirable, to manufacturing of structural components, where minimal adhesion and adhesive wear are often desired. Modeling of adhesion at different material interfaces from first principles has largely focused on computing the work of separation, $W_{sep}$, which is the reversible work required to separate an interface into two free surfaces (neglecting plastic and diffusional degrees of freedom[1]). Specific interface couples that have been modeled are: BeO/diamond,[2] Al/$\beta$-SiC,[3] Al/AlN,[4] Nb/sapphire,[1] Al/$\alpha$-$Al_2O_3$,[5] Al/WC,[6] Al/VN,[7] and Cu/diamond.[8] In general, $W_{sep}$ provides a useful measure of the strength with which two materials adhere to one another; however, it offers no detailed information about adhesive transfer due to an applied strain. In addition to knowing $W_{sep}$, it is important to know how the interfacial strength compares with the cohesive strength of the constituent materials and the only way to accomplish this is by imposing loads that lead to fracture.

We chose to study Al/diamond interfaces due to their broad applications, including Schottky diodes, field-effect transistors,[9] and in-plane gate transistors.[10] Another application that has received less attention is the design of adhesion-mitigating coating materials for Al forming. In these processes, nascent aluminum adheres to the tool: this leads to process termination. Various coatings have been applied to tool surfaces to inhibit adhesive transfer but most of these are largely unsuccessful.[11,12]

Experimental study of adhesion of Al and diamond is extremely challenging since it is difficult to keep Al from oxidizing even in ultra high vacuum conditions.[13] In reported sessile drop measurements, pure Al droplets wet diamond with work of adhesion values in the 1.0–1.2 $J/m^2$ range.[14] At the present time, there are no published fundamental studies of Al/diamond adhesion in a controlled environment that show how H-terminated diamond affects adhesion, like Cu/diamond.[15]

It is therefore the purpose of the present paper to present the first calculations of adhesion and adhesive transfer at Al/diamond interfaces using density functional theory. We first predicted that the freshly cleaved C(111)-1×1 rather than the reconstructed C(111)-2×1 leads to the lowest interfacial energy with Al. We then focused on computing $W_{sep}$ for Al(111)/C(111)-1×1 to represent the clean Al/diamond interface and Al(111)/C(111)-1×1:H. Finally we explored adhesive transfer by subjecting our interfaces to a series of tensile strain increments. The first principles simulations revealed new atomic-scale details of the interfacial separation process for each interface and provided a stress-strain relation for decohesion of the interfaces. This relation can inform decohesion processes at the continuum level with atomistic scale information.[16]

The Vienna *ab initio* Simulation Package (VASP)[17,18] was used to calculate the ground state energy and geometry of each interface. The generalized gradient approximation (GGA) of Perdew and Wang[19] was used for the exchange-correlation energy functional. Potentials constructed with the projector-augmented wave method[20] were used for C and H with core radii of 0.873 and 0.582 Å, respectively. A norm-conserving pseudopotential[21,22] with a cutoff radius of 0.96 Å was used for Al since its cutoff energy is closest to that of the other elements in the cell. The electronic degrees of freedom were converged to $10^{-5}$ eV/cell, and the Hellman-Feynman forces were relaxed to less than 0.05 eV/Å. Energy convergence of 1–2 meV/atom was obtained with 12 **k** points in the irreducible part of the brillouin zone and 400-eV plane wave cutoff energy.

The 13% lattice mismatch between Al and diamond precluded the construction of interfaces with perfect coherency (i.e., with surface Al and C atoms directly above each other). To minimize the mismatch, we used four C atoms per unit cell layer in C(111) and three Al atoms per unit cell layer of Al(111), and overlapped Al $\langle 11\bar{2}0\rangle$ with diamond $\langle 10\bar{1}0\rangle$. This reduced the mismatch to less than 2% such that we ignored misfit dislocations. Inversion symmetry was enforced in all cases to ensure that the two interfaces were identical and the interfacial energy was uniquely defined. This also precluded a dipole moment in the cell and nonphysical electrostatic coupling between periodic images. Figure 1(a) shows this partially coherent interface wherein only Al1 sits above a C atom, and Al2 and Al3 sit at the center of three C atoms, and above a C atom in the second diamond layer, respectively. We also investigated a fully incoherent interface, in which Al atoms lie above holes in both the first and second layers of C(111). The change in $W_{sep}$ was less than 0.5% for both the clean and H-terminated diamond. We focused, therefore, only on the partially coherent interface,

 

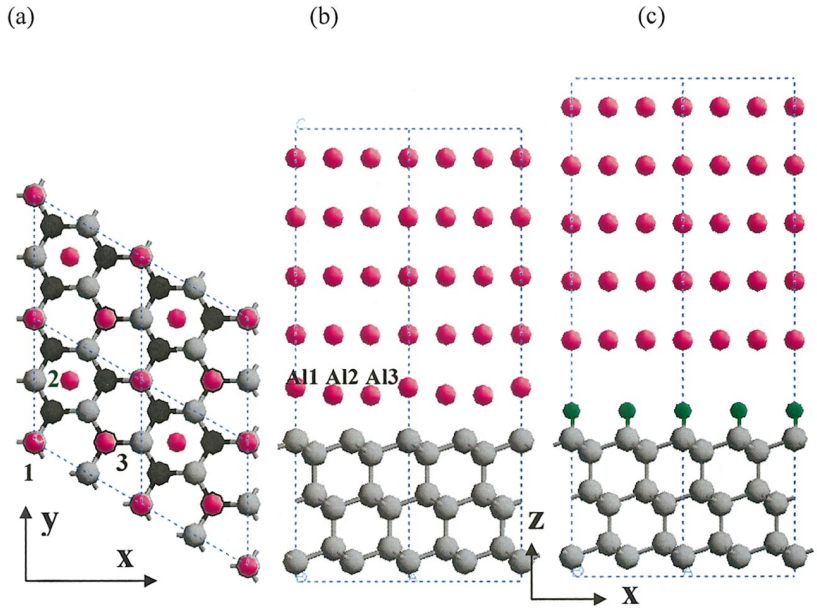


FIG. 1. (Color) Relaxed interfaces. (a) and (b) Projection of Al/C-1×1 ($a=b=5.027$ Å, $c=34.815$ Å) along $z$ and $y$, respectively. (c) Projection of Al/C-1×1:H ($a=b=5.018$ Å, $c=40.075$ Å) along $y$. Atom colors: Al, pink; C, gray (first layer) and black (second layer); H, green.

since it contains the strongest interfacial bonding. A convergence of the interfacial energy to less than 0.001 J/m$^2$ was found for the cell with 12-layer C(111) and ten-layer Al(111) slabs. Both the cell volume and atomic coordinates were optimized to get the relaxed interface structure and $W_{sep}$. Note that we shall omit (111) in the interface designations from this point onwards.

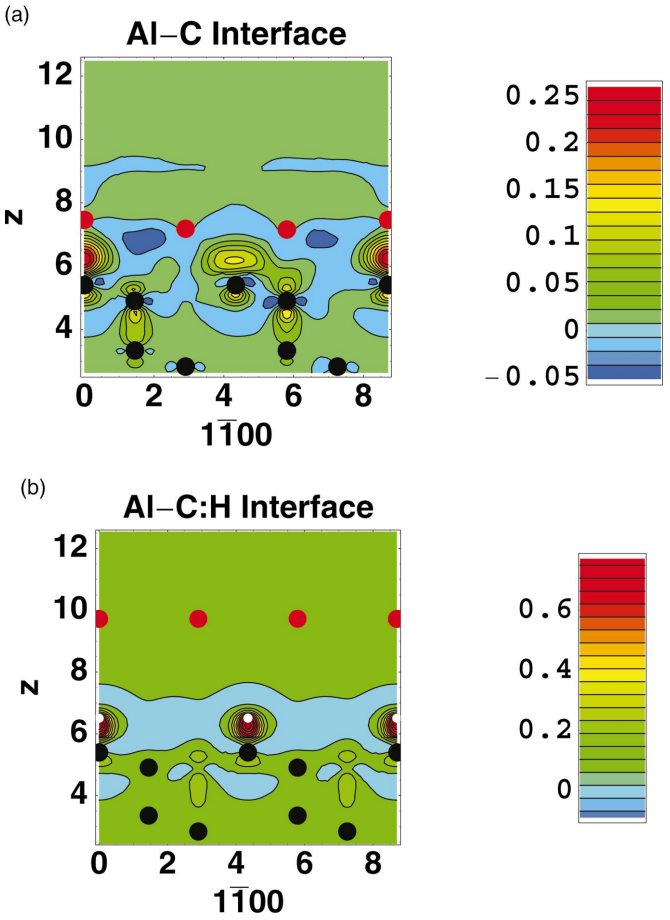


FIG. 2. (Color) Charge density differences ($\rho$/Å$^3$) along relaxed interfaces. (a) Al/C-1×1. (b) Al/C-1×1:H, with red, black, and white representing atomic positions of Al, C, and H, respectively.

A cleaved clean C(111) surface with single dangling bonds is unstable, and undergoes a 2×1 reconstruction.[9,23] We computed a 5.66 J/m$^2$ surface energy for C(111)-1×1, and 3.35 J/m$^2$ for the Pandey reconstructed[24] C(111)-2×1 surface, so the reconstruction lowers the surface energy by 2.31 J/m$^2$. However, the interfacial energy of Al/C-2×1 exceeds that of Al/C-1×1 by 1.43 J/m$^2$, with the former being 3.78 J/m$^2$ and the latter being 2.35 J/m$^2$. This implies that diamond dereconstructs upon exposure to Al to form stronger interface bonds, and the Al/C-1×1 interface is much more likely to be found experimentally. We therefore focused our study on Al/C-1×1 as the energetically favorable interface structure of Al and clean diamond. For Al/C-1×1, we computed the work of separation, $W_{sep}=4.08$ J/m$^2$, which drops to 1.81 J/m$^2$ upon reconstruction of the free diamond surface. Hydrogen terminated C(111) is found in as-grown CVD diamond.[9] We calculated a surface energy of 0.035 J/m$^2$ for a H-terminated diamond surface in a $CH_4$ ambient, which is the source gas in CVD diamond growth. For Al/C-1×1:H, we computed $W_{sep}=0.02$ J/m$^2$.

Optimized atomic arrangements of the relaxed interfaces are shown in Figs. 1(b) and 1(c). The first Al layer at the interface is rippled along the Al/C-1×1 interface [Fig. 1(b)], since Al1 moved away from the clean diamond surface, while Al2 and Al3 moved towards the diamond surface. The average distance between the Al and diamond at the interface was 1.86 Å. The average interlayer spacings in the first three layers of the Al slab were $D_{1\text{-}2}=2.22$ Å, $D_{2\text{-}3}=2.25$ Å, and $D_{3\text{-}4}=2.27$ Å. At the Al/C-1×1:H interface [Fig. 1(c)], the Al surface layer did not ripple, and the average distance between the Al and H layers at the interface increased to 3.21 Å, which is larger than the 2.33 Å interlayer spacing of Al(111). Wang and Smith[8] observed a similar repulsion of Cu by H-terminated diamond. We noted a decrease in the

(a)

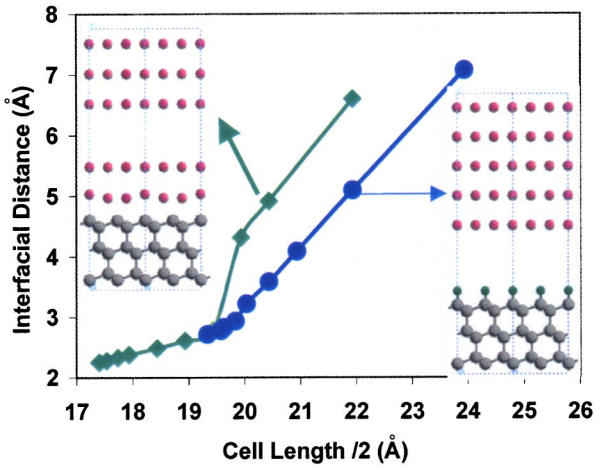


(b)

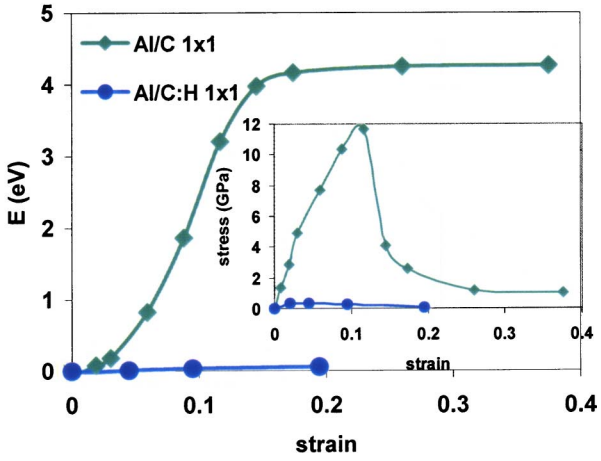


FIG. 3. (Color online) (a) Variation of interfacial distance with half-cell length. The fractured interface structures are shown as insets. (b) Variation of energy and stress with strain.

separation to 2.64 Å when optimizing with the local density approximation (LDA). The larger separation at the GGA-optimized interface is therefore due, in part, to underbinding. However, the smaller LDA separation does not significantly change either the $W_{sep}$, or the adhesive transfer with the H-terminated diamond surface.

To examine interface electronic structure, we plotted charge density differences for the optimized interface structures in the $(1\bar{1}00)$ plane in Fig. 2. For Al/C-1×1 [Fig. 2(a)], the interfacial Al/C bonds draw electrons from the Al (both surface and second layers) and diamond. The region between the coherent Al and C pair gained the most charge, demonstrating strongest bonding at the interface. Comparing the partial density of states for these two atoms with bulk atoms, we found that this strong bond came from Al and diamond *p* states at the interface, and the diamond surface shows local metallic character. We also computed the electron localization function,[25] which verified that the coherent interface bonds are indeed strongly covalent. The incoherent Al and C pairs also formed covalent bonds, which are weaker than those formed between the coherent pair. At the Al/C-1×1:H interface [Fig. 2(b)], electrons are drawn from the diamond to form strong covalent bonds between H and diamond, and there is no electron density between the H and Al.

Adhesive transfer was explored through the application of tensile strain increments to each cell. Starting with the minimum energy structure as the reference state, the interface couples were uniformly elongated at a set strain increment, followed by a minimization of all atoms to obtain the relaxed structure. The strain was then incremented and the process continued up to the point where two free surfaces formed. During the simulations, the strain was applied only along the *z* direction (perpendicular to the interface), while the cell lengths along the *x* and *y* directions were fixed.

The insets to Fig. 3(a) show the fractured interface structures for both cases, where the two free surfaces are at least 5 Å apart. Adhesive transfer occurred in Al/C-1×1, in which two layers of Al adhered to the diamond surface. This result is consistent with the correspondingly large $W_{sep}$. The H-terminated diamond and Al interface separated exactly at Al/C-1×1:H, due to the very weak bonding. In Fig. 3(a), we tracked the average interlayer distance between the fractured surfaces with respect to half of the cell length, which also can be interpreted as the system strain. We note from Fig. 3(a) that interfacial separation is not a continuous process for Al/C-1×1 since there are three distinct regimes in the curve. In the first regime, which extends from the original cell half-length of 17.4 Å (0% strain) to 19.4 Å (11.6% strain), all material is elastically stretched. In the second regime, which extends from 19.5 to 20 Å, the applied tensile stress exceeds the tensile yield stress of Al, and a large jump in the interlayer distance occurs (due to the onset and ultimate decohesion of the Al) as two (new) free surfaces are formed. In the third regime, wherein the slope of the interface displacement vs cell half-length is unity, the cell strain is localized at the fracture surfaces. If the interface failure involves bond breaking, the interfacial separation involves a jump prior to full separation. This jump to separation phenomenon has some similarity with the jump to contact process found by Smith *et al.*[26] In both cases, the interface bonds (bonding or debonding) lead to a jump in the interface separation. In contrast, the interfacial distance at Al/C-1×1:H is a smooth line with slope of unity during the separation process. No jump to separation is observed, which indicates no debonding during separation.

Figure 3(b) shows our computed energies and stresses for Al/C-1×1 and Al/C-1×1:H after each strain increment. Since fracture occurred inside the Al(111) slab as Al/C-1×1 was strained, failure resulted from the decohesion of the softer of the two materials. The work of decohesion, which we define as the energy difference (per unit surface area) between the fractured system and the interface structure at a zero stress state, was computed to be 1.56 $J/m^2$. If the fracture occurred exactly at the interface, as assumed when computing $W_{sep}$, it requires 4.08 $J/m^2$ to separate. $W_{sep}$ is therefore 2.5 times larger than the work of decohesion: this

reveals that it is energetically more favorable for the system to fracture within the Al slab than at the interface. We also calculated the work of decohesion to be 2.25 J/m$^2$ with one Al transfer layer and 1.60 J/m$^2$ with three Al transfer layers. We have tested the possibility of one or two Al transfer layers to the reconstructed diamond surface and found these structures to have higher energies of 1.37 and 1.54 J/m$^2$, respectively, and hence to be energetically unfavorable relative to the two Al transfer layers in Al/C-1×1. These confirmed that transfer of two Al layers corresponds to a global energy minimum. For Al/C-1×1:H, the energy change is close to zero: this is consistent with the very small $W_{sep}$. The maximum tensile strength we calculated for Al/C-1×1 is 12 GPa, but the stress needed to separate Al/C-1×1:H is less than 0.4 GPa: this latter value is 30 times lower than the ideal interfacial strength computed for Al/C-1×1.

Due to the small model size, no plastic deformation was allowed and the theoretical cohesive strength can be calculated via $\sigma_{max}=\sqrt{E\gamma/d}$, where $E$ is Young's modulus, $\gamma$ is the surface energy, and $d$ is the interplanar spacing along the tensile axis.[27] Using our VASP-computed values of $E=72.3$ GPa, $d=4.04$ Å, and $\gamma=0.76$ J/m$^2$ for Al, we find $\sigma_{max}=15.3$ GPa. The maximum tensile strength for Al/C-1×1 is 12 GPa, which is less than the theoretical tensile strength of bulk Al due to the effect of interface bonds. This is indicated in Fig. 2(a) wherein electrons transferred to the interface from the second layer of the Al slab, leading to weaker bonds between the second and third layers of the Al slab. Thus we define the interface strength as the stress associated with incipient separation at or near the interface, to distinguish the ideal strength of the interface structure from the cohesive strength of the bulk material.

In addition to the work of adhesion measurements cited earlier, two experiments are of significance to the present work and serve as a backdrop for qualitative comparison. Hollman *et al.*[11] measured very low friction coefficients and wear rates in dry sliding tests involving CVD-diamond coated cemented carbide drills against Al. However, Schmid and Hector[28] observed nascent Al adhesion to nanometer-size pyramidal diamond indenters in dry asperity abrasion processes. At first sight, it seems that Al adhesion to the pyramidal diamond indenters but not to the diamond coating is contradictory. However, the indenter and coating materials had completely different surface structures, the (111) surface cut from diamond probably had a clean surface. On the other hand, the diamond coating grown in the CVD process was H passivated.[9] These observations are in general agreement with our observation that Al adheres to a clean diamond surface but not to H-passivated diamond.

In summary, we found that the Al/C-1×1 interface had the lowest interfacial energy, which implies that it is the energetically favorable interface of Al and clean diamond, and we computed $W_{sep}$ to be 4.08 J/m$^2$; H-passivation of the diamond surface reduced $W_{sep}$ to 0.02 J/m$^2$. Electronic structure analysis showed strong covalent bonding between Al and C, but no bonds exist between Al and the H-passivated diamond surface. Under uniform tensile strain, the clean Al/diamond interface fractured within the Al slab at 12 GPa, with two layers of Al transferring to the diamond surface. The work of decohesion for this process was computed to be 1.56 J/m$^2$. The Al/H-terminated-diamond interface separated at the interface under 0.4 GPa, and no adhesive transfer occurred. Existing experimental results in ambient provide qualitative support of the results predicted herein.

The authors wish to acknowledge Dr. Erich Wimmer and Dr. John R. Smith for several stimulating discussions, and Dr. T.W. Capehart and Dr. Y.T. Cheng for providing valuable insights on diamond coating applications.

[1] I. G. Batyrev, A. Alavi, and M. W. Finnis, Phys. Rev. B **62**, 4698 (2000).
[2] W. R. L. Lambrecht and B. Segall, J. Mater. Res. **7**, 696 (1992).
[3] J. Hoekstra and H. Kohyama, Phys. Rev. B **57**, 2334 (1998).
[4] S. Ogata and H. Kitagawa, J. Jpn. Inst. Met. **60**, 1079 (1996).
[5] D. J. Siegel, L. G. Hector, Jr., and J. B. Adams, Phys. Rev. B **65**, 085415 (2002).
[6] D. J. Siegel, L. G. Hector, and J. B. Adams, Jr., Surf. Sci. **498**, 321 (2002).
[7] D. J. Siegel, L. G. Hector, and J. B. Adams, Jr., Acta Mater. **50**, 619 (2002).
[8] X. Wang and J. R. Smith, Phys. Rev. Lett. **87**, 186103 (2001).
[9] H. Kawarada, Surf. Sci. Rep. **26**, 205 (1996).
[10] J. A. Garrido *et al.*, Appl. Phys. Lett. **82**, 988 (2003).
[11] P. Hollman *et al.*, Wear **179**, 11 (1994).
[12] A. Erdemir, Surf. Coat. Technol. **146–147**, 292 (2001); K.-H. Habig, *ibid.* **76–77**, 540 (1995); M. Berger and S. Hogmark, *ibid.* **149**, 14 (2002).
[13] K. Miyoshi *et al.*, NASA Technical Report TM-1998-206638, April 1998.
[14] Y. V. Naidich, in *Progress in Surface and Membrane Science*, edited by D. A. Cadenhead and J. F. Danielli (Academic Press, New York, 1981), Vol. 14; A. R. Ford and A. E. White, Chem. Eng. (Rugby, U.K.) **166**, 61 (1963).
[15] S. V. Pepper, J. Vac. Sci. Technol. **20**, 643 (1982).
[16] H. H. M. Cleveringa, E. Van der Giessen, and A. Needleman, J. Mech. Phys. Solids **48**, 1133 (2000).
[17] G. Kresse and J. Hafner, Phys. Rev. B **49**, 14251 (1994).
[18] G. Kresse and J. Furthmüller, Comput. Mater. Sci. **6**, 15 (1996).
[19] J. P. Perdew *et al.*, Phys. Rev. B **46**, 6671 (1992).
[20] P. E. Blöchl, Phys. Rev. B **50**, 17953 (1994).
[21] A. M. Rappe *et al.*, Phys. Rev. B **41**, 1227 (1990).
[22] L. Kleinman and D. M. Bylander, Phys. Rev. Lett. **48**, 1425 (1987).
[23] A. Scholze *et al.*, Phys. Rev. B **53**, 13725 (1996).
[24] K. C. Pandey, Phys. Rev. B **25**, 4338 (1982).
[25] A. D. Becke and K. E. Edgecombe, J. Chem. Phys. **92**, 5397 (1990).
[26] J. R. Smith *et al.*, Phys. Rev. Lett. **63**, 1269 (1989).
[27] N. H. Macmillan, J. Mater. Sci. **7**, 239 (1972).
[28] S. R. Schmid and L. G. Hector, Jr., Wear **215**, 257 (1997).